Title
Organelle Size Scaling of the Budding Yeast Vacuole by Relative Growth and Inheritance

Journal
Current Biology, 26(9)

ISSN
0960-9822

Authors
Chan, Yee-Hung M
Reyes, Lorena
Sohail, Saba M
et al.

Publication Date
2016-05-01

DOI
10.1016/j.cub.2016.03.020

Peer reviewed

HHS Public Access

Author manuscript

Curr Biol. Author manuscript; available in PMC 2017 May 09.

Published in final edited form as:

Curr Biol. 2016 May 9; 26(9): 1221–1228. doi:10.1016/j.cub.2016.03.020.

Organelle size scaling of the budding yeast vacuole by relative growth and inheritance

Yee-Hung M. Chan[1,2,†], **Lorena Reyes**[3], **Saba M. Sohail**[3], **Nancy K. Tran**[3], and **Wallace F. Marshall**[1,2,*]

[1]University of California, San Francisco, Department of Biochemistry and Biophysics, 600 16th St., San Francisco, CA, 94158, USA

[2]Center for Systems and Synthetic Biology, 600 16th St., San Francisco, CA, 94158, USA

[3]San Francisco State University, Department of Biology, 1600 Holloway Ave., San Francisco, CA, 94132, USA

Summary

It has long been noted that larger animals have larger organs compared to smaller animals of the same species, a phenomenon termed scaling [1]. Julian Huxley proposed an appealingly simple model of "relative growth"—in which an organ and the whole body grow with their own intrinsic rates [2]—that was invoked to explain scaling in organs from fiddler crab claws to human brains. Because organ size is regulated by complex, unpredictable pathways [3], it remains unclear if scaling requires feedback mechanisms to regulate organ growth in response to organ or body size. The molecular pathways governing organelle biogenesis are simpler than organogenesis, therefore organelle size scaling in the cell provides a more tractable case for testing Huxley's model. We ask the question: Is it possible for organelle size scaling to arise if organelle growth is independent of organelle or cell size? Using the yeast vacuole as a model, we tested whether mutants defective in vacuole inheritance, *vac8Δ* and *vac17Δ*, tune vacuole biogenesis in response to perturbations in vacuole size. In *vac8Δ/vac17Δ*, vacuole scaling increases with the replicative age of the cell. Furthermore, *vac8Δ/vac17Δ* cells continued generating vacuole at roughly constant rates even when they had significantly larger vacuoles compared to wild-type. With support from computational modeling, these results suggest there is no feedback between vacuole biogenesis rates and vacuole or cell size. Rather, size scaling is determined by the relative growth rates of the vacuole and the cell, thus representing a cellular version of Huxley's model.

[*]Corresponding author, wallace.marshall@ucsf.edu.

[†]Current affiliation: San Francisco State University, Department of Biology, 1600 Holloway Ave., San Francisco, CA, 94132, USA, yhmchan@sfsu.edu

Author contributions

Y.-H. M. C. designed this project and performed experiments. Y-H. M. C, L. R., S. M. S., and N. K. T. and W. F. M. analyzed data. Y.-H. M. C. and W. F. M. wrote the paper.

Results and Discussion

Vacuole-to-cell size scaling in vacuole inheritance mutants increases with cell replicative age

Do cells tune biogenesis pathways to maintain a particular vacuole-to-cell size ratio? To answer this question, we utilize mutants defective in vacuole inheritance to perturb vacuole size independently of biogenesis. Vacuoles labeled with Vph1p-GFP were imaged in wild-type (BY4741 parent strain), and in *vac8Δ/vac17Δ* (vacuole inheritance mutants) yeast strains (Fig. 1A/Fig. S1A). Vacuole inheritance involves the myosin-to-vacuole adapter proteins, Vac8p and Vac17p [4], and so *vac8Δ/vac17Δ* inheritance mutants are unable to segregate vacuoles between mother and bud [5]. As Class I inheritance mutants, *vac8Δ* and *vac17Δ* create one of the strongest forms of vacuole inheritance defects [6] that ultimately requires the bud to grow a new vacuole de novo [7].

vac8Δ/vac17Δ buds contained relatively little vacuole, in agreement with described results [6]. Qualitative observations suggested that vacuole size in these strains diverges from strongly from wild-type. We therefore quantified vacuole volume and surface area—which have been shown to scale with cell volume in wild-type strains [8]—using our previously published surface reconstruction method [9]. Both the vacuole's lumenal volume and membrane surface play critical roles in vacuole function. The former houses many of the organelle's degradative and homeostatic functions [10], and the latter contains proteins involved in transport [11] and signaling [12]. From the perspective of size control, changes in vacuole surface area depend on the flux of membrane to the organelle as determined by positive and negative biogenesis mechanisms, including anterograde [13]/retrograde [14] trafficking pathways and autophagy [15]. Vacuole volume, on the other hand, is capable of changing independently of these biogenesis pathways through fusion/fission mechanisms [16, 17], changes to organelle shape [5], and other mechanisms.

Scaling plots of vacuole size vs. cell size for wild-type, *vac8Δ/vac17Δ* (Fig. 1B&C/Fig. S1B&C), showed that perturbing inheritance in the mutant strains led to a breakdown of scaling, with *vac8Δ/vac17Δ* showing a larger range and increased values of both vacuole volume and surface area than wild-type. Vac8p has a multitude of functions in the cell, including involvement in the TOR signaling pathway [18] and vacuole association with other organelles [19]. The consistency in results between *vac8Δ* and *vac17Δ* strains, however, confirms that our observations relate to their common impacts on inheritance.

Since inheritance is linked to cell division, we hypothesized that the scaling divergence in *vac8Δ/vac17Δ* could result from increased dependence of vacuole content on replicative age. We inferred mother generational age using bud scar counting. In wild-type cells, vacuole surface and volume size scaling trends from 1st to 4th generation showed only minor differences as the cells aged (Fig. 2A&B). While mother cells' vacuole scaling trends show minor changes, bud cells seem to show very consistent vacuole size scaling regardless of the mother's replicative age (Fig. S2A–D). In contrast, mutant cells showed significant increases in vacuole size scaling ratio from generation to generation (*vac8Δ*: Fig. 2C&D, *vac17Δ*: Fig. S2E&F)—i.e. older cells have larger vacuoles than younger cells of the same size.

To quantify the divergence in vacuole-to-cell size scaling, vacuole volume- and vacuole surface area-to-cell volume ratios were calculated for individual cells, then averaged within generations (Fig. 2E&F, Fig. S2G&H). 1st generation wild-type and *vac8Δ* cells showed similar average scaling ratios, both with respect to volume and to surface area. However, *vac8Δ* cells showed larger generational increases in vacuole volume- and surface area-to-cell volume scaling ratios.

Vacuole surface area scaling showed similar trends in *vac17Δ* (Fig. S2G). *vac17Δ* vacuole volume scaling, (Fig. S2H) however, seems to begin at a smaller ratio that wild-type in 1st generation cells. This ratio increases by generation, and it surpasses wild-type levels by 3rd generation. The continued increase into 4th generation indicates that *vac17Δ* vacuole also accumulate in an age-dependent fashion.

Cell and vacuole growth rates in wild-type and vac8Δ

The *vac8Δ/vac17Δ* mutants provide us with a way to test whether cells and their vacuoles can recover from abnormal scaling. Since the vacuole is a compartment in the endomembrane system, its growth depends on membrane trafficking [20], and perturbing trafficking pathways can have quantifiable effects on vacuole-to-cell size scaling [8]. The organelle undergoes fusion and fission which impact its copy number and volume [16, 17], and recent modeling of experimental distributions indicates that vacuole copy number experiences minimal regulation [21].

Although vacuoles were smaller in *vac8Δ* buds (Fig. S1D–I), they attained wild-type scaling levels during their 1st generation after division (Fig. 2E&F), consistent with results observed for the *vac17Δ* mutant by Jin and Weisman [7]. This recovery implied that either *vac8Δ* cell or organelle growth rates, or both, were adjusted to restore the correct scaling. Vacuole then grew even larger by 2nd–4th generations (Fig. 2E&F), even when the vacuole in the mother was overly large, which implied that any feedback mechanisms that allowed recovery in the first G1 do not function in subsequent generations to maintain proper vacuole size. To test how growth rates may have been regulated, we imaged log-phase yeast cells and vacuoles at ten minute intervals using time-resolved microscopy.

1st and 2+ generation mothers were identified and imaged through at least one full division cycle (Fig. 3A, Fig. S3A). These traces were synchronized such that t=0 corresponds to the timepoint with the first appearance of a bud. Mean values and standard deviations of cell and vacuole sizes were calculated for each timepoint. Both wild-type and *vac8Δ* cells increased in volume during G1 (Fig. 3B&C, blue shading, *vac17Δ*: Fig. S3B) and continued to grow during budding (Fig. 3B&C, pink shading, *vac17Δ*: Fig. S3B), with growth localized to the bud (Fig. S4A–C). After cytokinesis, total cell volume decreased sharply as the newborn daughter split apart from its older mother. Then, the older mother cell would usually begin producing its next bud within 10–20min in wild-type, with a commensurate increase in total cell volume (Fig. 3B, no shading).

In wild-type cells, vacuoles grew in surface area (Fig. 3D) and volume (Fig. 3F) with growth trends qualitatively similar to cell growth. Vacuoles' membrane surface grew in the mother during G1, and then in the bud during budding (Fig. S4D). (At t=10m, average vacuole size

appears to decrease, but this is likely due method errors in measuring the elongated segregation structures that the vacuole forms in early budding [5]). Upon cytokinesis, total vacuole size decreased sharply as the bud and its vacuole separated from the mother (because after cytokinesis the bud is no longer included in the total), then grew again as the cell entered the next cell cycle. This pattern of vacuole growth was observed for wild-type cells of all generations. 1st and 2+ bud vacuoles grew at similar rates, even though mother vacuoles increased in size with replicative age (Fig. S4A), supporting the idea that mothers of all generations construct buds with similar organelle size [22].

Vacuoles in 1st generation *vac8Δ* mothers also grew during G1 (surface area: Fig. 3E, volume: Fig. 3G, *vac17Δ*: Fig. S3C&D). However, during budding, *vac8Δ* buds did not develop an ole until 40–50min—much later than in wild-type—which reflects the inheritance defect in this strain (Fig. S4E, *vac17Δ*: Fig. S4F). Interestingly, *vac8Δ* mother vacuoles continued to grow during budding and into the second cell cycle as well (Fig. 3E&G, S4G, *vac17Δ*: Fig. S3C&D, Fig S4H). Even though 2+ generation *vac8Δ* mothers all started with larger vacuoles than 1st generation, their vacuoles also generally grew during budding, with growth again localized to the mothers (Fig. S4G, *vac17Δ*: Fig. S4H).

Scaling recovers in newborn but not 2+ generation vac8Δ cells

Vacuole volume- and vacuole surface area-to-cell size scaling ratios revealed how vacuole-to-cell size scaling changes during the cell cycle. For wild-type, average scaling ratios in 1st generation total cells remained roughly constant through G1, budding, and past cytokinesis for total cells (Fig. 3H) and mothers and buds (Fig. S4I). In *vac8Δ* (Fig. 3I & K, *vac17Δ*: Fig. S3E&F), the scaling ratios in newborn cells were initially less than in wild-type. In agreement with previous studies [7], the ratios increased steadily during the first G1, then tended to plateau upon budding at a value similar to the wild-type average. This result is consistent with the finding that 1st generation *vac8Δ* cells show similar population scaling trends to wild-type cells (Fig. 2E). Upon cytokinesis in *vac8Δ* strains, vacuole-to-cell size scaling ratios increased dramatically due to loss of the bud cell volume. 2+ generation mothers therefore started budding with higher vacuole-to-cell size ratios compared to wild-type, and scaling continues to increase in 2+ generation mothers during budding (Fig. S4J, *vac17Δ:* Fig. S4K). These results indicate that in *vac8Δ*, repeated cycles of vacuole synthesis and accumulation in the mother cause progressive increases in vacuole size scaling ratios with replicative age.

Vacuole-to-cell size scaling trends reflect the relationship between organelle and cell growth rates. We therefore measured these rates in 1st and 2+ generation cells. In wild-type cells, vacuole volume exhibited non-uniform growth rates (Fig. 3F), in a large part due to vacuole shape changes. Vacuole volume increases in the mother during budding (Fig. S4L), concomitant with a reduction in the number of vacuole compartments in the mother (Figure S4M), even though vacuole surface area tends to remain constant in the mother (Fig. S4D). This linked change in volume and compartment number, combined with a lack of change in total surface area, suggests that vacuole fusion may itself lead to changes vacuole volume independent of membrane biogenesis (Fig. S4). In *vac8Δ* cells, vacuole volume grew more uniformly (Fig. 3G, *vac17Δ*: Fig. S3D). In contrast to the non-uniform increases seen at the

level of vacuole volume, we found that vacuole surface area increased steadily at a constant rate in both wild-type and *vac8Δ* (Fig. 3D&E, *vac17Δ*: Fig. S3C). In wild-type, during budding, bud cells and vacuoles grew steadily, but the mother cells and vacuoles showed little net change in size such that most of the growth was taking place in the bud (Fig. S4D). The balance between bud cell and vacuole growth rates maintained overall scaling in the cell (Fig. 3H&J).

In *vac8Δ*, for the vacuole-to-cell size ratio to increase in newborn mothers' first G1, either cell or vacuole growth rates, or both, must be altered. Since the vacuole's membrane surface provides a direct measure of vacuole biogenesis, and since vacuole volume but not surface area was observed to be sensitive to vacuole fusion, we conducted these comparisons using vacuole surface area. Vacuole growth rates for 1st generation wild-type and *vac8Δ* cells did not differ significantly in G1 (surface area, p=0.4, Student's t-test, see Fig. 3; *vac17Δ*: p=0.8, see Fig. S3). In contrast to the lack of impact on vacuole growth rate, cell growth rate was significantly reduced in *vac8Δ* cells ($p<10^{-3}$, Student's t-test, see Fig. 3; *vac17Δ:* p=0.02, see Fig. S3), leading to the increased scaling ratio in G1. Upon budding, total *vac8Δ* cell growth rate increased but was still slightly slower than wild-type ($p<10^{-3}$, Student's t-test, see Fig. 3; *vac17Δ:* p=0.06, see Fig. S3), and total vacuole surface area growth rate was not significantly different from wild-type (p=0.5, Student's t-test, see Fig. 3; *vac17Δ:* p=0.7, see Fig. S3). These growth rates maintained the total vacuole-to-cell size scaling ratio in *vac8Δ* at a value similar to wild-type. Upon cytokinesis, the scaling ratio increased sharply, reflecting the loss of the bud cell's volume. The slower growth rate, and the longer budding time of *vac8Δ*, may be due in part to Vac8p's role in a cell-cycle checkpoint related to TOR signaling at the mother's vacuole [7].

By 2nd generation, *vac8Δ* cells had a greater vacuole-to-cell size scaling ratio than in 1st generation (Fig. 3I&K). At this point, vacuole surface area continued growing at a rate that was not statistically significantly different from 1st generation *vac8Δ* cells (p=0.7, Student's t-test, see Figs. 3 and S4; *vac17Δ:* p=0.8, see Figs. S3 and S4), showing that vacuole biogenesis in *vac8Δ* was not altered to compensate for aberrant accumulation in the mother. Even when the amount of vacuole in the total cell was many times that of normal, vacuole continued to be produced at the start of budding (Fig. S4G, *vac17Δ*: Fig S4H). Thus we did not observe an alteration in vacuole growth rate, either when the vacuole content was less than normal in newborn *vac8Δ* mother cells, or when it was greater than normal in older *vac8Δ* cells. These findings are contrary to what one would expect if membrane trafficking and other vacuole biogenesis mechanisms were under feedback control as a function of the vacuole quantity, and they are consistent with a relative growth model to generate vacuole-to-cell size scaling.

Modeling of cell and vacuole growth to achieve scaling

To determine whether population-wide vacuole-to-cell size scaling can arise from relative growth rates in the absence of feedback, we implemented a theoretical model of cell and vacuole growth in asymmetrically dividing cells (Fig. 4A). To account for natural variation in cell and vacuole growth rates, we evaluated model predictions using Monte Carlo simulations to predict population-wide scaling distributions (Supplemental Materials and

Methods, Table S1). This model resembles Huxley's relative growth model, but one difference is that mother and daughter cells reenter the budding cycle after division. The model contains no feedback term to modify cell or vacuole growth rates in response to cell or vacuole size. Output populations showed very similar vacuole-to-cell size scaling trends to the experimental data, demonstrating that scaling can arise from constant cell and organelle growth without the need for explicit feedback (Fig. 4B, left). Increasing growth rate variance led to decreased population-wide scaling strength, as evidenced by decreasing R^2-coefficients (Fig. 4B, middle and right).

Inheritance was represented as a term distributing newly synthesized vacuole between mother and bud. For simulations of wild-type strains, net vacuole growth was restricted solely to the bud. When the population was separated by replicative age, different generations of cells showed overlapping scaling trends (Fig. 4C, left). To test the effect of inheritance defects, net growth of the vacuole was either randomly distributed between mother and bud or fully restricted to the mother. In these cases, the population showed increasing divergence with respect to replicative age (Fig. 4C, middle and right). These results show that for size scaling to remain consistent between generations in an asymmetrically dividing cell, organelle growth must be localized to where the cell is growing. Since these models demonstrate that scaling can arise in the absence of feedback mechanisms to tune organelle or cell growth, we conclude that vacuole size scaling in yeast can be explained by Huxley's relative growth model.

Alternative models of organelle size regulation

Relative growth models are commonly used to describe the growth of organs and bodies to establish scaling. In cases where growth is exponential, different exponential growth rates (referred to as "allometric growth") for an organ versus the whole body lead to power law scaling of organ size to body size. At the cellular level, organelle-to-cell size scaling has been observed for the nucleus [23, 24], mitotic spindle [25–27][25–27](Good et al., 2013; Hazel et al., 2013; Wilbur and Heald, 2013)[25–27][25–27], flagella [28, 29], centrosome [30], mitochondria [22], and vacuoles [8, 9, 31]. Scaling may allow organelle functional capacity to meet increased demand in growing cells [29, 32–34]. Many models of size regulation have been discovered that regulate organelle size and establish scaling. For instance, organelle growth can depend on cell size through the establishment of a limiting pool of components as is observed for centrosome assembly [35], or the cell-geometry dependent sequestration of a microtubule destabilizer in mitotic spindle assembly [27].

We have shown that in *vac8Δ* and *vac17Δ*, vacuole growth does not exhibit regulation with respect to the vacuole-to-cell size ratio. However, this finding does not rule out other possible regulatory mechanisms. In other examples of organelle size regulation, organelle growth rate depends in part on cell size such that the organelle grows faster in larger cells, presumably due to a higher overall biosynthetic capacity [27, 34]. However, we can rule out this possibility, as vacuole growth rates remain constant even during cell growth when cell size is constantly increasing (Fig. 3E). Furthermore, instantaneous vacuole growth rates show no correlation with cell size (Fig S4N).

Another possible model is that vacuole growth rate is dependent on the cell's growth rate, as both ultimately rely on cellular metabolism. For instance, in cells grown to diauxic shift—during which cell division ceases and cell growth slows—vacuoles do not grow indefinitely, but maintain a size scaling that is comparable to log-phase cells [9]. Indeed, any example of relative organelle and cell growth would be consistent with such a model.

While vacuole size increases during the generations we observed, ultimately the vacuole cannot exceed the volume of the cell. As volume becomes constrained, for the vacuole to grow further in surface area, it must fragment into ever larger numbers of compartments, which may explain why the organelle is multi-lobed in *vac8Δ/vac17Δ* and other Class I inheritance mutant strains [6]. Other classes of inheritance mutants show different vacuole morphologies [36], which may indicate a different mode of vacuole size regulation. The increasing size of the vacuole in *vac8Δ* may play a role in the strain's reduced replicative fitness [37], and this and other functional impacts of vacuole size regulation remain a rich area for exploration.

In *vac8Δ* and *vac17Δ*, it is unclear if cells are unable to respond to the excess vacuole. It may be that inheritance is the primary mechanism to remove excess vacuole, or that Vac8p/Vac17p act in other pathways, including vacuole biogenesis pathways, that are needed for recovery. In these cases, the mutant strains would be inherently unable to deal with the perturbed organelle size, but the wild-type still could. Another model to explain the divergence in vacuole size is that the cell is unresponsive to changes in the mother's vacuole, but may continue producing vacuole in an attempt to overcome the inheritance defect in the bud. These intriguing possibilities will be explored in future manuscripts.

Supplementary Material

Refer to Web version on PubMed Central for supplementary material.

Acknowledgments

We thank Kurt Thorn and the Nikon Imaging Center at UCSF for microscopy support and the members of the Marshall lab for helpful comments. Y.-H. M. C. acknowledges the support of the Herbert Boyer Postdoctoral Fellowship and the NIH NRSA award 1F32GM090442-01A1, and W.F.M. acknowledges the support of NIH grants R01 GM097017 and P50 GM081879.

References

1. Thompson, D'Arcy Wentworth. On Growth and Form. Bonner, John Tyler, editor. Cambridge, England: Cambridge University Press; 1992.
2. Huxley, J. Problems of Relative Growth. Mineola, New York: Dover Publications Inc.; 1972.
3. Lui JC, Baron J. Mechanisms Limiting Body Growth in Mammals. Endocr Rev. 2011; 32:422–440. [PubMed: 21441345]
4. Hill KL, Catlett NL, Weisman LS. Actin and myosin function in directed vacuole movement during cell division in Saccharomyces cerevisiae. J Cell Biol. 1996; 135:1535–1549. [PubMed: 8978821]
5. Weisman LS. Yeast Vacuole Inheritance and Dynamics. Annu Rev Genet. 2003; 37:435–460. [PubMed: 14616069]
6. Wang YX, Zhao H, Harding TM, Gomes de Mesquita DS, Woldringh CL, Klionsky DJ, Munn AL, Weisman LS. Multiple classes of yeast mutants are defective in vacuole partitioning yet target vacuole proteins correctly. Mol Biol Cell. 1996; 7:1375–1389. [PubMed: 8885233]

7. Jin Y, Weisman LS. The vacuole/lysosome is required for cell-cycle progression. eLife. 2015:e08160.
8. Chan YHM, Marshall WF. Organelle size scaling of the budding yeast vacuole is tuned by membrane trafficking rates. Biophys J. 2014; 106:1986–1996. [PubMed: 24806931]
9. Chan, YHM.; Marshall, WF. Threshold-free method for three-dimensional segmentation of organelles. 2012. p. 822529–822529–7Available at: http://dx.doi.org/10.1117/12.909278 [Accessed September 17, 2013]
10. Klionsky DJ, Herman PK, Emr SD. The fungal vacuole: composition, function, and biogenesis. Microbiol Rev. 1990; 54:266–292. [PubMed: 2215422]
11. Russnak R, Konczal D, McIntire SL. A Family of Yeast Proteins Mediating Bidirectional Vacuolar Amino Acid Transport. J Biol Chem. 2001; 276:23849–23857. [PubMed: 11274162]
12. Wurmser AE, Emr SD. Phosphoinositide signaling and turnover: PtdIns(3)P, a regulator of membrane traffic, is transported to the vacuole and degraded by a process that requires lumenal vacuolar hydrolase activities. EMBO J. 1998; 17:4930–4942. [PubMed: 9724630]
13. Raymond CK, Howald-Stevenson I, Vater CA, Stevens TH. Morphological classification of the yeast vacuolar protein sorting mutants: evidence for a prevacuolar compartment in class E vps mutants. Mol Biol Cell. 1992; 3:1389–1402. [PubMed: 1493335]
14. Bryant NJ, Piper RC, Weisman LS, Stevens TH. Retrograde Traffic Out of the Yeast Vacuole to the TGN Occurs via the Prevacuolar/Endosomal Compartment. J Cell Biol. 1998; 142:651–663. [PubMed: 9700156]
15. Yorimitsu T, Klionsky DJ. Autophagy: molecular machinery for self-eating. Cell Death Differ. 2005; 12:1542–1552. [PubMed: 16247502]
16. Wickner W, Haas A. YEAST HOMOTYPIC VACUOLE FUSION: A Window on Organelle Trafficking Mechanisms. Annu Rev Biochem. 2000; 69:247–275. [PubMed: 10966459]
17. Michaillat L, Baars TL, Mayer A. Cell-free reconstitution of vacuole membrane fragmentation reveals regulation of vacuole size and number by TORC1. Mol Biol Cell. 2012; 23:881–895. [PubMed: 22238359]
18. Tang F, Peng Y, Nau JJ, Kauffman EJ, Weisman LS. Vac8p, an Armadillo Repeat Protein, Coordinates Vacuole Inheritance With Multiple Vacuolar Processes. Traffic. 2006; 7:1368–1377. [PubMed: 16824055]
19. Krick R, Mühe Y, Prick T, Bredschneider M, Bremer S, Wenzel D, Eskelinen EL, Thumm M. Piecemeal microautophagy of the nucleus: Genetic and morphological traits. Autophagy. 2009; 5:270–272. [PubMed: 19182523]
20. Bryant NJ, Stevens TH. Vacuole Biogenesis in Saccharomyces cerevisiae: Protein Transport Pathways to the Yeast Vacuole. Microbiol Mol Biol Rev. 1998; 62:230–247. [PubMed: 9529893]
21. Mukherji S, O'Shea EK. Mechanisms of organelle biogenesis govern stochastic fluctuations in organelle abundance. eLife. 2014; 3:e02678. [PubMed: 24916159]
22. Rafelski SM, Viana MP, Zhang Y, Chan YHM, Thorn KS, Yam P, Fung JC, Li H, Costa L da F, Marshall WF. Mitochondrial network size scaling in budding yeast. Science. 2012; 338:822–824. [PubMed: 23139336]
23. Jorgensen P, Edgington NP, Schneider BL, Rupes I, Tyers M, Futcher B. The size of the nucleus increases as yeast cells grow. Mol Biol Cell. 2007; 18:3523–3532. [PubMed: 17596521]
24. Neumann FR, Nurse P. Nuclear size control in fission yeast. J Cell Biol. 2007; 179:593–600. [PubMed: 17998401]
25. Good MC, Vahey MD, Skandarajah A, Fletcher DA, Heald R. Cytoplasmic Volume Modulates Spindle Size During Embryogenesis. Science. 2013; 342:856–860. [PubMed: 24233724]
26. Hazel J, Krutkramelis K, Mooney P, Tomschik M, Gerow K, Oakey J, Gatlin JC. Changes in Cytoplasmic Volume Are Sufficient to Drive Spindle Scaling. Science. 2013; 342:853–856. [PubMed: 24233723]
27. Wilbur JD, Heald R. Mitotic spindle scaling during Xenopus development by kif2a and importin α. eLife. 2013; 2:e00290. [PubMed: 23425906]
28. Wemmer, KA.; Marshall, WF. Flagellar Length Control in Chlamydomonas— A Paradigm for Organelle Size Regulation. In: Jeon, Kwang W., editor. International Review of Cytology.

Academic Press; 2007. p. 175-212.Available at: http://www.sciencedirect.com/science/article/pii/S0074769606600041 [Accessed September 17, 2013]

29. Chan YHM, Marshall WF. Scaling properties of cell and organelle size. Organogenesis. 2010; 6:88–96. [PubMed: 20885855]
30. Brangwynne CP. Phase transitions and size scaling of membrane-less organelles. J Cell Biol. 2013; 203:875–881. [PubMed: 24368804]
31. Uchida M, Sun Y, McDermott G, Knoechel C, Le Gros MA, Parkinson D, Drubin DG, Larabell CA. Quantitative analysis of yeast internal architecture using soft X-ray tomography. Yeast Chichester Engl. 2011; 28:227–236.
32. Chan YHM, Marshall WF. How cells know the size of their organelles. Science. 2012; 337:1186–1189. [PubMed: 22955827]
33. Levy DL, Heald R. Mechanisms of Intracellular Scaling. Annu Rev Cell Dev Biol. 2012; 28:113–135. [PubMed: 22804576]
34. Goehring NW, Hyman AA. Organelle Growth Control through Limiting Pools of Cytoplasmic Components. Curr Biol. 2012; 22:R330–R339. [PubMed: 22575475]
35. Decker M, Jaensch S, Pozniakovsky A, Zinke A, O'Connell KF, Zachariae W, Myers E, Hyman AA. Limiting Amounts of Centrosome Material Set Centrosome Size in C. elegans Embryos. Curr Biol. 2011; 21:1259–1267. [PubMed: 21802300]
36. Weisman LS, Emr SD, Wickner WT. Mutants of Saccharomyces cerevisiae that block intervacuole vesicular traffic and vacuole division and segregation. Proc Natl Acad Sci. 1990; 87:1076–1080. [PubMed: 1689059]
37. Tang F, Watkins JW, Bermudez M, Gray R, Gaban A, Portie K, Grace S, Kleve M, Craciun G. A lifespan-extending form of autophagy employs the vacuole-vacuole fusion machinery. Autophagy. 2008; 4:874–886. [PubMed: 18690010]

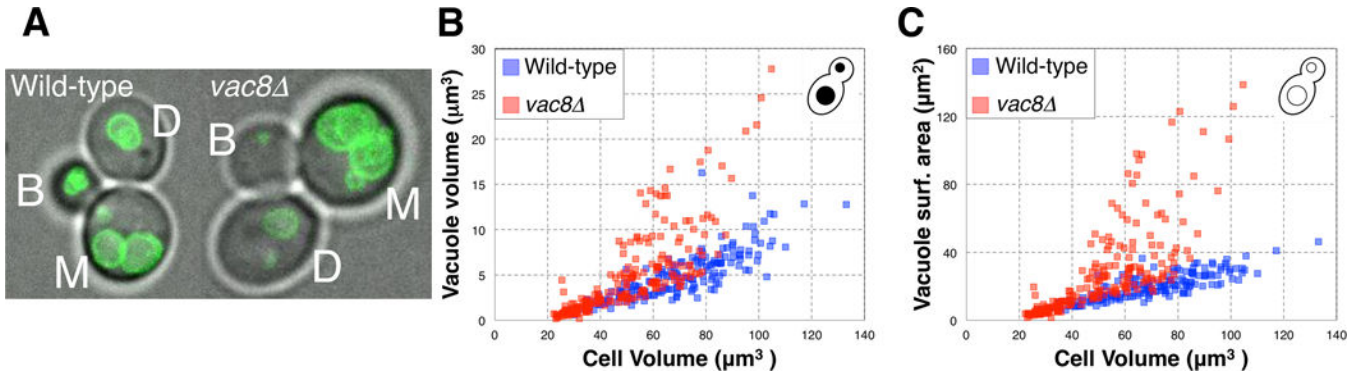

Figure 1. Vacuole inheritance defect causes divergence in vacuole-to-cell size scaling

(A) Representative images of wild-type and *vac8Δ* cells (brightfield) and vacuoles (Vph1p-GFP). In each image, the cells are arranged in a frequently-observed pattern where a 2+ generation mother, M, has produced a 1st generation daughter, D, in the previous cell cycle, and is currently producing a new bud, B. (B) Vacuole volume and (C) vacuole surface area vs. cell volume scaling plots for wild-type (blue) and *vac8Δ* (red) cells. Wild-type and *vac8Δ* scaling plots are significantly different from one-another for both volume and surface area ($p<0.001$, comparison of regression lines.) See also Figure S1.

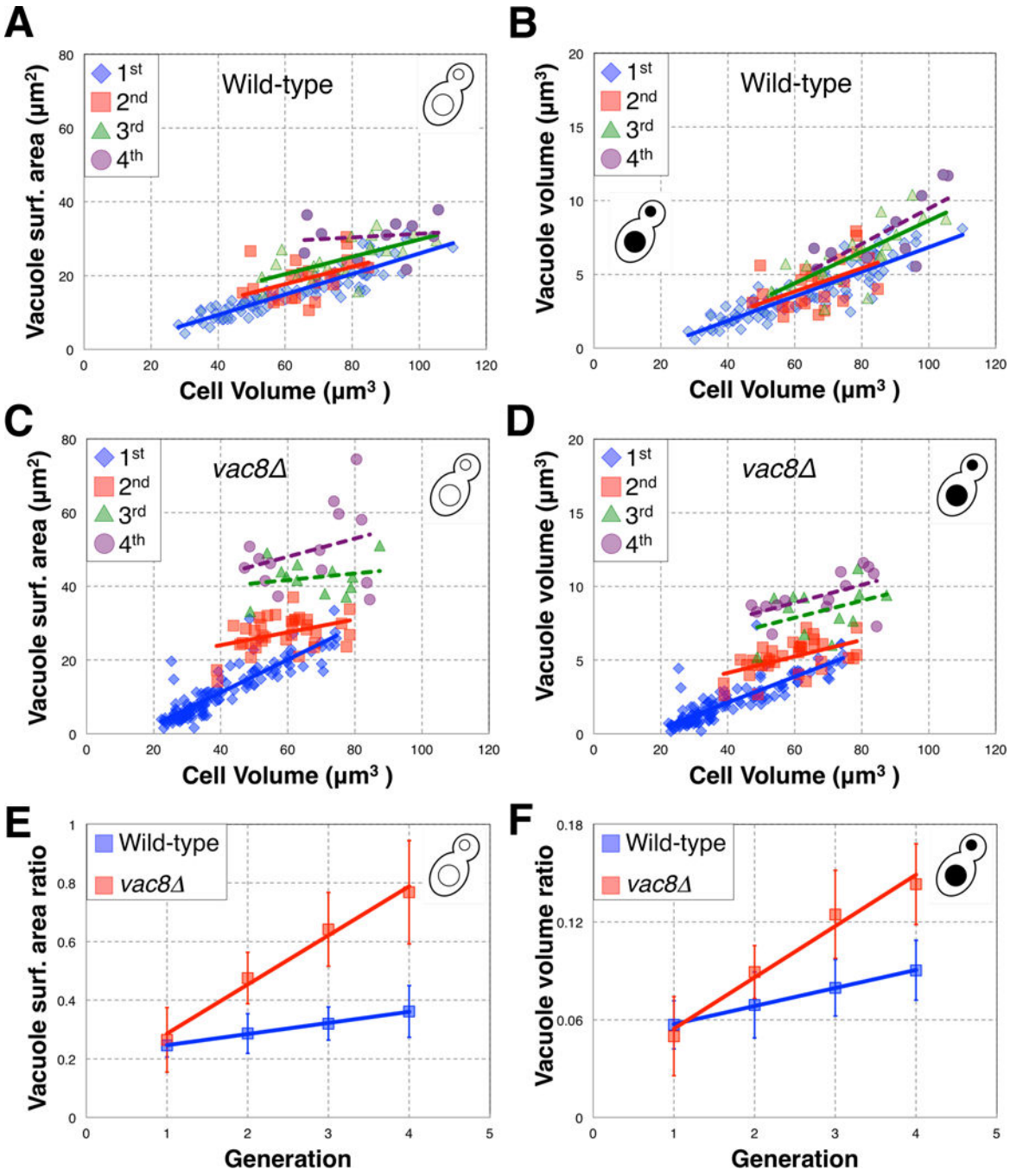

Figure 2. Vacuole size scaling defects in inheritance mutants increase with replicative age

(A) Wild-type vacuole surface area; (B) wild-type vacuole volume; (C) *vac8Δ* vacuole surface area; and (D) *vac8Δ* vacuole volume vs. cell volume scaling plots were separated according to generational age. Lines represent best linear fits (solid, p-value<0.05; dashed, p-value>0.05). (F) Vacuole surface area- and (G) vacuole volume-to-cell volume ratios were averaged for cells binned by replicative age. Lines represent best linear fits, and error bars represent standard deviations. *vac8Δ* cells (red) show a much steeper increase in scaling ratio than wild-type (blue). See also Figure S2.

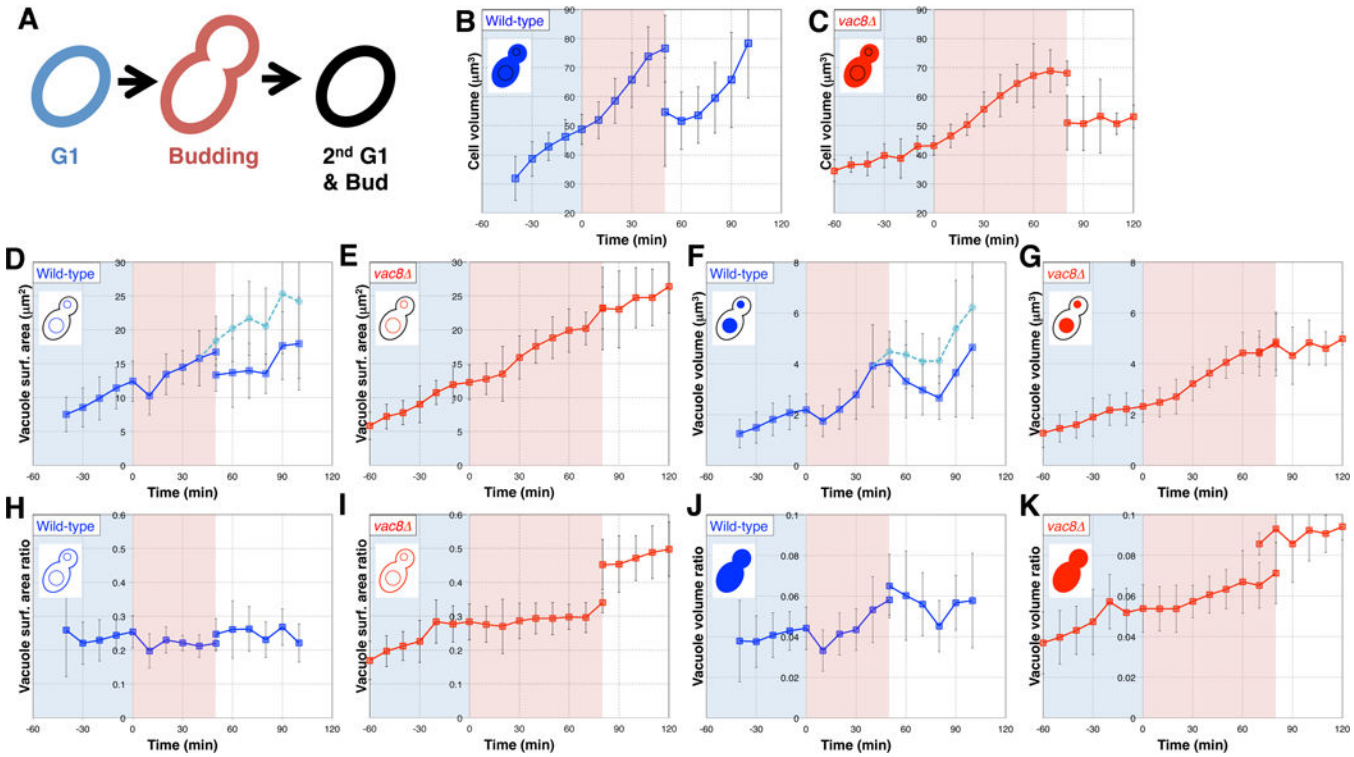

Figure 3. Wild-type and *vac8Δ* vacuoles grow at similar rates regardless of the vacuole-to-cell size scaling ratio

(A) Total cell (mother cell and its bud) and total vacuole sizes were measured at 10min intervals for 1st generation mothers undergoing their first G1 (blue shading) and budding (red shading) followed by their second cell cycle (no shading). Timecourse plots (B)–(K) show average values at each timepoint with error bars depicting standard deviations. (B) Wild-type (n=10) and (C) *vac8Δ* (n=10) average cell volume plotted against time. (D) Wild-type and (E) *vac8Δ* average vacuole surface area plots. (F) Wild-type and (G) *vac8Δ* average vacuole volume plots. In (D) & (F), the cyan line corresponds to the sum of vacuole sizes in the now 2nd generation mother and her newborn 1st generation daughter. This represents the cumulative amount of vacuole growth. Vacuole surface area-to-cell volume ratios were calculated averaged for each timepoint for (H) wild-type and (I) *vac8Δ* cells. Vacuole volume-to-cell volume ratios were calculated and averaged for each timepoint for (J) wild-type and (K) *vac8Δ* cells. See also Figures S3 and S4.

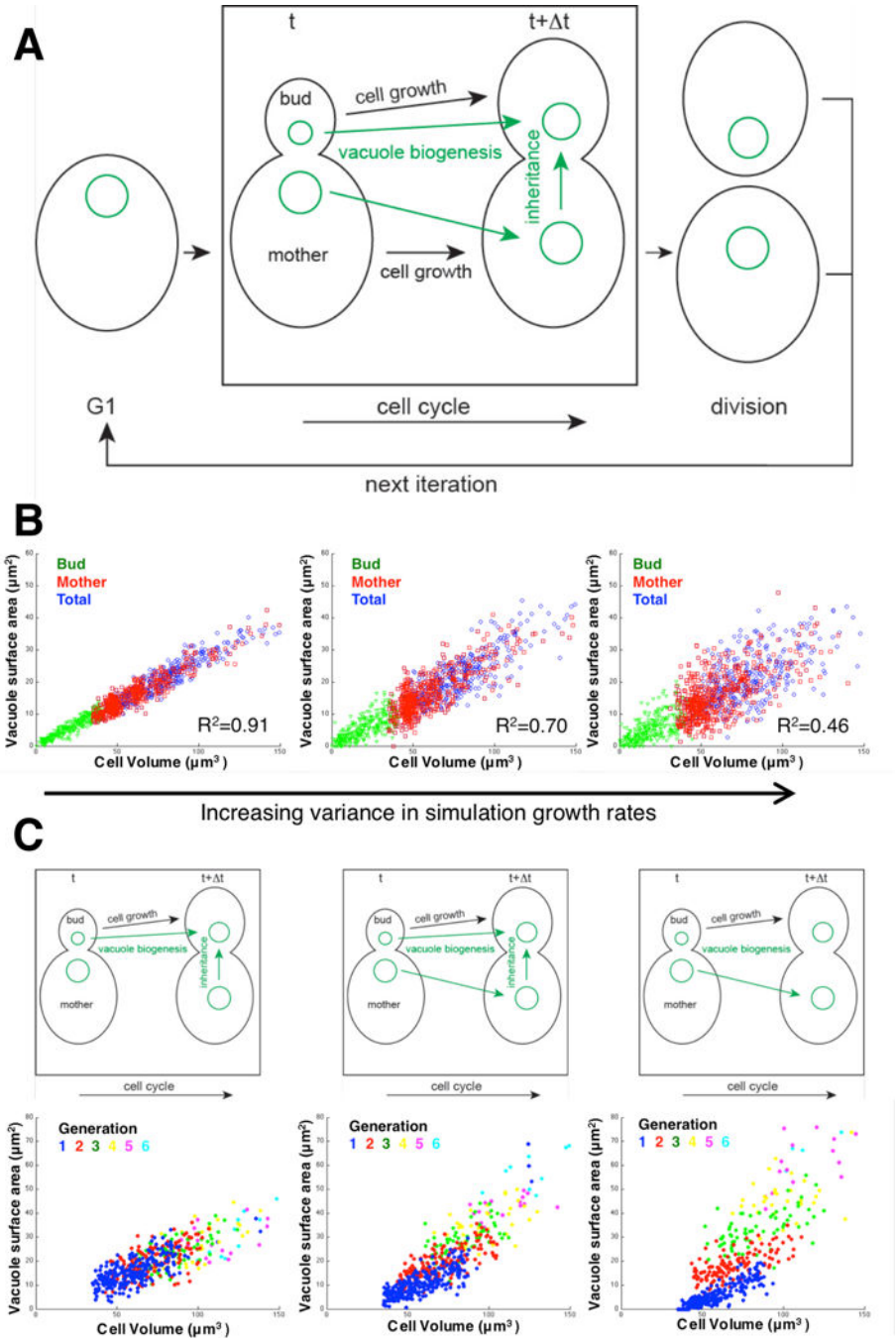

Figure 4. Model of cell growth, vacuole growth, and vacuole inheritance

(A) Illustration of the simulation of cell and vacuole growth. In G1, a mother cell and its vacuole grow. The mother enters the cell cycle in which growth is restricted to the bud. When the bud reaches a certain size, division can occur, producing two mothers that enter another iteration of the cell cycle. (B) Using constant cell and vacuole growth rates produces populations that are similar to wild-type, and increasing variance in these rates leads to decreasing R^2-coefficients in the population scaling plots. (C) Vacuole growth can be localized to the bud (left, wild-type), mother (*vac8Δ*, right), or randomly distributed between

both cells (middle). Changes to inheritance lead to divergence in the scaling plots with respect to replicative age. See also Table S1.